Concept of the Energy-Dependent Temperature for Direct Langevin Dynamics Simulations of Rare Events in Systems with Arbitrary High Energy Barriers

Dmitry Berkov, Elena K. Semenova, and Natalia L. Gorn

General Numerics Research Lab, Leutragraben 1, D-07743 Jena, Germany

We suggest an algorithm which allows single-stage direct Langevin dynamics simulations of transitions over arbitrarily high energy barriers. For this purpose, we propose a concept of the energy-dependent temperature (EDT): near the energy minima this temperature is high, but it tends toward room temperature for energies approaching the barrier value. In the resulting algorithm simulation time required for the computation of the escape rate over the barrier does not increase with barrier height. Switching times computed via our EDT algorithm agree very well with those obtained with the forward flux sampling (FFS). As the simulation time required by our method does not increase with the energy barrier, we achieve a very large speed-up compared even to our strongly optimized version of FFS (and all other multistage algorithms). In addition, our approach is free from the instability occurring in all multistage "climbing" methods where a product of a large number of transition probabilities between the interfaces must be computed.

Introduction.—Studies of systems with many mestastable states separated by energy barriers and evaluation of escape rates Γ over these barriers are highly important tasks arising in many areas of physics, chemistry, molecular biology, and material science by studying, e.g., catalytic reactions, diffusion in solids, phase transitions, information lifetime, etc. [1–8]. This task is much more difficult than the computation of the energy barrier height ΔE [3,9–12], because the system dynamics in the vicinity of the saddle point is very complicated.

The simplest analytical formula for Γ—the Arrhenius law $\Gamma = \nu_{att} \exp(\Delta E / k_B T)$ (ν_{att} being the "attempt frequency")—has a fundamental drawback [13,14], as it does not include the system damping. The most advanced analytical expression for Γ for arbitrary damping was derived in Ref. [15]. In magnetism, the formalism from Ref. [15] was successfully applied to transitions between two energy minima of a single-domain particle in Refs. [14,16,17]. However, an analytical approach cannot be used for strongly interacting many-particle systems (or continuous bodies); an example of such systems is magnetic particles with sizes larger than the micromagnetic length [18] which have substantially nonuniform magnetization states. Hence, general numerical methods for the evaluation of Γ are clearly necessary.

Straightforward Langevin dynamics (LD) is suitable for small barriers only ($\Delta E / k_B T \leq 10$), because its simulation time grows exponentially with ΔE. Hence, most methods for studying transitions over high barriers are based on a gradual "climbing" towards the saddle point starting from an energy minimum. Among them, the most successful is the forward flux sampling (FFS) [19–22]. In FFS the phase space between the energy minima is divided into N interfaces $\{\lambda_i\}$ and the transition probabilities $w(\lambda_i \rightarrow \lambda_{i+1}) \equiv w_i$ between the interfaces are computed. The escape rate is then obtained by multiplying the product of all w_i's by the flux from the starting minimum through the first interface. In micromagnetics, FFS was applied for magnetization switching in columnar structures [23–25] and skyrmions [26].

Computational time for one FFS run is proportional to ΔE, because for larger barriers one needs more interfaces N to maintain the accuracy of computed w_i's. In addition, a large time effort is required to optimize positions of interfaces in the coordinate space [21,22] (we could eliminate this effort [27] by placing interfaces equidistantly in the energy space). Another serious problem of FFS is the instability by the multiplication of $N \gg 1$ numerically evaluated probabilities w_i [28].

Thus, a new class of numerical methods which could compute the switching rate using only *single-stage* LD simulations for *any* barriers is highly desirable. Here we present such a method introducing the concept of the energy-dependent effective temperature. We show that it allows fast and accurate direct LD simulations of transitions over arbitrarily high barriers with the simulation time which does not increase with ΔE. An extended version of this research is presented in Ref. [28].

Concept of the energy-dependent temperature (EDT).— Direct LD simulations of transitions over high barriers fail because the system spends the majority of its time near its energy minima, and the probability to reach the region near
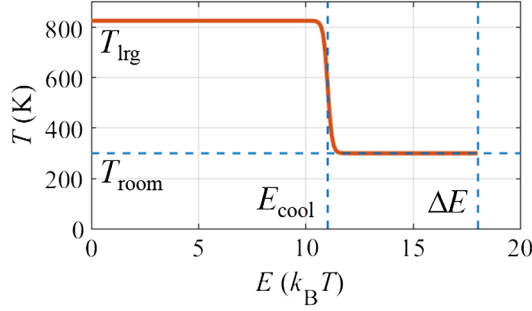
FIG. 1.   Energy-dependent temperature (1) for $\Delta E = 18 k_B T$; $a_{\rm lrg} = 4$, $b_{\rm cool} = 7$.

a saddle is exponentially small [$p \sim \exp(-\Delta E/k_B T)$]. To eliminate this drawback, we suggest to perform LD simulations using energy-dependent temperature $T(E)$, which is equal to the room temperature $T_{\rm room}$ for energies near the saddle point and is much higher than $T_{\rm room}$ for energies considerably lower than ΔE. For this purpose, we use the functional dependence,

$$T(E) = \frac{T_{\rm room} + T_{\rm lrg}}{2} + \frac{T_{\rm room} - T_{\rm lrg}}{2} \tanh\left(\frac{E - b_{\rm cool} k_B T}{\Delta_T}\right) \tag{1}$$

(see Fig. 1), where the finite width $\Delta_T = (0.1 - 1.0) k_B T$ ensures a smooth transition between "hot" and "cold" regions to avoid numerical instabilities of LD trajectories.

Temperature $T_{\rm lrg}$ and the "cooling" energy $E_{\rm cool} = \Delta E - b_{\rm cool} \cdot k_B T_{\rm room}$ should provide a relatively high probability $p_{\rm cool}$ to occupy states near $E_{\rm cool}$, from which a system will overcome the remaining energy barrier at $T \approx T_{\rm room}$. We have found that $p_{\rm cool} \approx \exp(-E_{\rm cool}/k_B T_{\rm lrg})$ should lie in the range 0.002–0.02 to achieve a sufficiently high occupation of these states, leading to the values $E_{\rm cool}/k_B T_{\rm lrg} = a_{\rm lrg} \approx 4$–$6$; results below are obtained for $a_{\rm lrg} = 4$.

Finally, $b_{\rm cool}$ controls the effective barrier height $\Delta E_{\rm eff} = \Delta E - E_{\rm cool} = b_{\rm cool} \cdot k_B T_{\rm room}$ to be overcome starting from $E_{\rm cool}$. The upper limit of $b_{\rm cool}^{\max} \approx 10$ is posed by standard LD simulations, for which $\Delta E_{\rm eff}/k_B T \leq 10$. Too low values of $b_{\rm cool}(< 5)$ lead to very frequent barrier crossings and problems by distinguishing "true" and "false" transitions [27]. Within this range $5 \leq b_{\rm cool} \leq 10$ we have used $b_{\rm cool} = 7$ for results presented here (see Ref. [28] for more details).

Clearly, for systems with $T(E)$ [Eq. (1)] numerous switchings will be observed in LD simulations for any barrier height, because the effective barrier to be overcome is always only $\Delta E^{\rm EDT} \simeq b_{\rm cool} k_B T$. Thus, $\tau_{\rm sw}$ for the system with EDT can be computed directly by dividing the physical LD simulation time by the number of true switchings: $\tau_{\rm sw}^{\rm EDT} = t_{\rm sim}/N_{\rm sw}$ [27]. The main problem is

how to establish the relation between $\tau_{\rm sw}^{\rm EDT}$ and the real switching time at a constant temperature $\tau_{\rm sw}^{\rm CT}$.

Relation between $\tau_{\rm sw}^{\rm EDT}$ *and* $\tau_{\rm sw}^{\rm CT}$.—For this purpose we use the same expression for the transition rate Γ as in FFS: for N virtual interfaces $\{\lambda_i, i = 1, ..., N\}$ between the basins **A** and **B** ($\lambda_1 \equiv \lambda_{\bf A}$, $\lambda_N \equiv \lambda_{\bf B}$), we have

$$\Gamma_{\bf A \to B} = \Phi_{\bf A}(T) \cdot \prod_{i=2}^{N-1} w_{i \to i+1}, \tag{2}$$

where $\Phi_{\bf A}$ denotes the flux out of the basin **A** [22,27].

Using Eq. (2) and recalling that $\tau_{\rm sw} = 1/\Gamma$, we obtain

$$\frac{\tau_{\rm sw}^{\rm CT}}{\tau_{\rm sw}^{\rm EDT}} = \frac{\Gamma_{\bf A \to B}^{\rm EDT}}{\Gamma_{\bf A \to B}^{\rm CT}} = \frac{\Phi_{\bf A}^{\rm EDT}(T = T_{\rm lrg})}{\Phi_{\bf A}^{\rm CT}(T = T_{\rm room})} \cdot r, \tag{3}$$

with r being the ratio of probability products,

$$r = \prod_{i=2}^{N-1} w_{i \to i+1}^{\rm EDT} / \prod_{i=2}^{N-1} w_{i \to i+1}^{\rm CT}, \tag{4}$$

so that the actual switching time (at $T = T_{\rm room}$) is

$$\tau_{\rm sw}^{\rm CT} = \tau_{\rm sw}^{\rm EDT} \cdot \frac{\Phi_A^{\rm EDT}}{\Phi_A^{\rm CT}} \cdot r. \tag{5}$$

In this expression, $\tau_{\rm sw}^{\rm EDT}$ in Eq. (5) and both fluxes Φ can be computed directly using LD EDT simulations. Thus, to obtain $\tau_{\rm sw}^{\rm CT}$, we need only a method to evaluate the ratio r (4). We point out that this method should have negligibly low computational cost, otherwise the EDT algorithm will not be any better than the standard FFS.

Markov chain formalism for EDT.—We shall compute the ratio (4) using the Markov chain (MCH) formalism [29]. We introduce the Markov chain with the states $\{1, ..., N\}$, corresponding to our interfaces $\{\lambda_1, ..., \lambda_N\}$ and *one-step* transition probabilities $p_{i \to i+1}$ and $q_{i \to i-1}$ between them. These probabilities form the one-step transition matrix $\hat{\bf P}$, which gives the change of the state occupations in a MCH after one step: $P_{i,i+1} = p_{i \to i+1}$ and $P_{i,i-1} = q_{i \to i-1}$.

To compute the total probabilities $w_{i \to i+1}$ in MCH formalism, we recall how they are computed in FFS: many trajectories are launched from the interface λ_i and simulated using LD until they either reach λ_{i+1} or return to **A**. Probability $w_{i \to i+1}$ is then defined as the fraction of trajectories arriving λ_{i+1}.

Hence the random process serving to obtain $w_{i \to i+1}$ terminates when the system reaches either the state 1 or $(i + 1)$. This means that it is described by the subset of $i + 1$ states of our full Markov chain. So for the computation of $w_{i \to i+1}$ we have a MCH of the length $(i + 1)$ with absorbing borders, and corresponding elements of its $\hat{\bf P}^{(i+1)}$ matrix are $P_{11}^{(i+1)} = P_{i+1,i+1}^{(i+1)} = 1$, $P_{12}^{(i+1)} = p_{1 \to 2} = 0$, and $P_{i+1,i}^{(i+1)} = q_{i+1 \to i} = 0$:

$$\hat{\mathbf{P}}^{(i+1)} = \begin{bmatrix} 1 & 0 & & & & \cdots & & 0 \\ q_{21} & 0 & p_{23} & & & & & \\ 0 & q_{23} & 0 & p_{34} & & & & \\ \vdots & & & \ddots & & & & \vdots \\ & & & & 0 & p_{i-1,i} & & \\ & & & & q_{i,i-1} & 0 & p_{i,i+1} & \\ 0 & & & & \cdots & & 0 & 1 \end{bmatrix}.$$

(6)

Next, we recall that $w_{i \to i+1}$ is computed by LD without restricting the simulation time. In the MCH language this means that we look for the probability that a system starting from the ith state will be found in the $(i + 1)$th state after an arbitrary large number of steps (equilibrium). Thus, we have to find the matrix $\hat{\mathbf{E}}^{(i+1)} = \lim_{k \to \infty}(\hat{\mathbf{P}}^{(i+1)})^k$, and the probability of interest is then given by the matrix element $w_{i \to i+1} = E_{i,i+1}^{(i+1)}$.

Importantly, the matrix $\hat{\mathbf{E}}^{(i+1)}$ can be computed very fast: diagonalizing the matrix $\hat{\mathbf{P}}^{(i+1)} = \hat{\mathbf{Q}}\,\hat{\mathbf{D}}\,\hat{\mathbf{Q}}^{-1}$, we obtain $\lim_{k \to \infty}(\hat{\mathbf{P}}^{(i+1)})^k = \lim_{k \to \infty}\hat{\mathbf{Q}}\hat{\mathbf{D}}^k\hat{\mathbf{Q}}^{-1}$. Hence we need only the limits $\lim_{k \to \infty} d_j^k$ for eigenvalues of $\hat{\mathbf{P}}^{(i+1)}$. As $\hat{\mathbf{P}}^{(i+1)}$ are the so-called stochastic matrices (the sum of elements of each row is one), all their eigenvalues obey the inequality $d_i \leq 1$, so these limits are either 0 or 1.

Assignment of one-step probabilities.—To assign $p_{i \to i+1}$ and $q_{i+1 \to i}$ for our MCH, we first establish the correspondence between its states and the energy landscape. In our EDT algorithm we use the same equidistant positioning of MCH states in the energy space (Fig. 2), as in Ref. [27], so that probabilities $w_{i \to i+1} \sim \exp(-(E_{i+1} - E_i)/kT)$ are approximately equal for all "uphill" interface pairs.

This interface placement allows us to assign the MCH probabilities using the detailed balance principle from thermodynamics [2]. Namely, one-step probabilities $p_{i \to j}$ and $q_{j \to i}$ are related to equilibrium probabilities to find the system in the corresponding states π_i and π_j via $\pi_i p_{i \to j} = \pi_j q_{j \to i}$. In equilibrium, the probabilities π are given by $\pi_i \simeq n_i \exp(-E_i/k_B T)$, where n_i is the density of

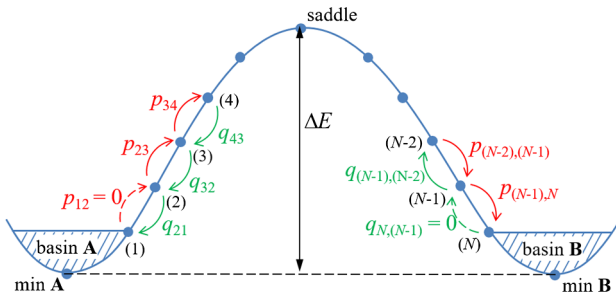states (DOS) at the energy E_i. Hence, $p_{i \to i+1}$ and $q_{i+1 \to i}$ should obey the relation

$$\frac{p_{i \to i+1}}{q_{i+1 \to i}} = \frac{\pi_{i+1}}{\pi_i} = \frac{n_{i+1}}{n_i}\exp\left(-\frac{\delta E_{i,i+1}}{k_B T}\right), \quad (7)$$

with $\delta E_{i,i+1} = E_{i+1} - E_i$. To satisfy this relation, we set

$$p_{i \to i+1} = \sqrt{\frac{n_{i+1}}{n_i}}\exp\left(-\frac{1}{2}\frac{\delta E_{i,i+1}}{k_B T}\right), \quad q_{i+1 \to i} = \frac{1}{p_{i \to i+1}}. \quad (8)$$

To evaluate n_{i+1}/n_i, we expand $n_{i+1} = n(E_{i+1})$ for small energy increments $\delta E_{i,i+1} \equiv \delta E$ near $E = E_i$, obtaining

$$\left(\frac{n_{i+1}}{n_i}\right)^{\pm 1/2} = 1 \pm \frac{\delta E}{2n_i}\frac{\partial n}{\partial E}\bigg|_{E=E_i}. \quad (9)$$

Thus, for energies where DOS $n(E)$ is nonsingular (i.e., E does not correspond to an extremum of a saddle point) we can set $n_{i+1}/n_i \approx 1$ for small $\delta E \to 0$. Finally, we have to normalize p's and q's so that $p_{i \to i+1} + q_{i \to i-1} = 1$.

Probabilities $p_{i \to i+1}$ as functions of the interface number i for $T = T(E)$ given by Eq. (1) exhibit [according to their definition (8)] a jump at the saddle point interface, where the energy difference $E_{i+1} - E_i$ changes its sign. In addition, p_i's rapidly change also around the interfaces corresponding to $E_{\text{cool}} = \Delta E - b_{\text{cool}}k_B T$ due to the temperature drop (see Ref. [28] for details).

Validation of the EDT algorithm.—Total MCH transition probabilities obtained from the one-step quantities p_i and q_i as $w_{i \to i+1} = E_{i,i+1}^{(i+1)}$ are shown in Fig. 3 (lines with
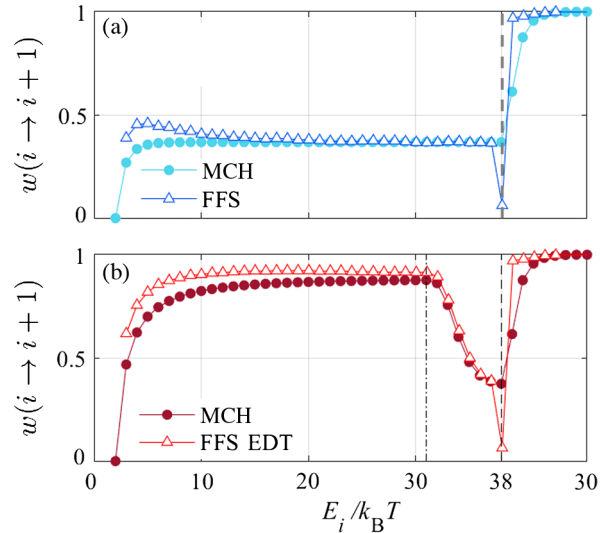

FIG. 2. Markov chain and energy landscape.

FIG. 3. Total transition probabilities $w_{i \to i+1}$ for FFS (open triangles) and MCH (closed circles) methods for the constant $T = 300$ K (a) and EDT given by Eq. (1) (b); here $\Delta E/k_B T = 38$ and $\delta E/k_B T = 1$.

circles). Their behavior can be better understood by comparing them to analogous quantities calculated by FFS with the same interfaces. First we note that the difference between $w_{i \to i+1}$ obtained by MCH and FFS for interfaces well below the saddle point is due to the rather large value of $\delta E = 1 k_B T$, so that neglecting the second term in the expansion (9) of $n(E)$ has a noticeable effect; this difference rapidly decreases with $\delta E \to 0$.

The most important feature of $w_{i \to i+1}$ seen in Fig. 3 both for $T = \mathrm{const}$ and EDT is the large discrepancy between MCH and FFS probabilities at and slightly above the saddle point energy ΔE. This discrepancy reflects the qualitative difference between the FFS and MCH methods. Namely, in FFS we evaluate $w_{i \to i+1}$ by LD simulations fully taking into account complicated system dynamics near the saddle point (i.e., back hopping) and peculiarities of FFS interfaces. In particular, for our macrospin the probability to reach the saddle point interface λ_s is especially small (large dips at $E_i = \Delta E$ on w_i dependencies for FFS), because in order to reach this interface, m_x projection should change its sign (see Refs. [27,28] for more details). For this reason the distance between λ_{s-1} and λ_s in the coordinate space is much larger than for preceding interface pairs, so that the probability $w(\lambda_{s-1} \to \lambda_s)$ is smaller. Further, $w_{i \to i+1}$ strongly increases after λ_s, because the probability to return to previous interfaces is very low. In contrast, for our MCH we merely compute the limit $\hat{\mathbf{E}}^{(i+1)} = \lim_{k \to \infty}(\hat{\mathbf{P}}^{(i+1)})^k$ where one-step probabilities p_i and q_i in $\hat{\mathbf{P}}$ have only a relatively small jump near the saddle, so that $w_{i \to i+1}$ changes in this region much slower than for FFS.

However—and this is the key point—the *ratio* of probabilities $w_{i \to i+1}^{\mathrm{EDT}}/w_{i \to i+1}^{\mathrm{CT}}$ should be the same (in the limit $\delta E \to 0$) for FFS and MCH methods for all interface energies, including the saddle point region.

This statement follows directly from the EDT construction (1), where $T(E) \to T_{\mathrm{room}}$ for $E \simeq \Delta E$. Because of this behavior, for one-step MCH probabilities (8) near the saddle point we have $p_{i \to i+1}^{\mathrm{EDT}} = p_{i \to i+1}^{\mathrm{CT}}$ (the same for q's). Hence, as long as b_{cool} is large enough to allow $w_{i \to i+1}$ to reach its steady-state value for $T = T_{\mathrm{room}}$ in the saddle point region, in this region we obtain $w_{i \to i+1}^{\mathrm{EDT}} = w_{i \to i+1}^{\mathrm{CT}}$. In the FFS method, probabilities w_i are obtained from LD simulations, which "feel" at each time integration step only the local temperature, so that we have $w_{i \to i+1}^{\mathrm{EDT}} = w_{i \to i+1}^{\mathrm{CT}}$ also for FFS.

Corresponding ratios $w_{i \to i+1}^{\mathrm{EDT}}/w_{i \to i+1}^{\mathrm{CT}}$ are plotted in Fig. 4. They agree for FFS and MCH methods very well for all interfaces—both far below the saddle (where only the local temperatures matter) and near the saddle point, where the system dynamics plays a decisive role in FFS. This means that the ratio r (4) required for the evaluation of τ_{sw} in EDT can be computed from the Markov chain method by diagonalizing the matrices $\hat{\mathbf{P}}^{(i+1)}$. Moreover, this ratio depends only on the function $T(E)$ and thus can
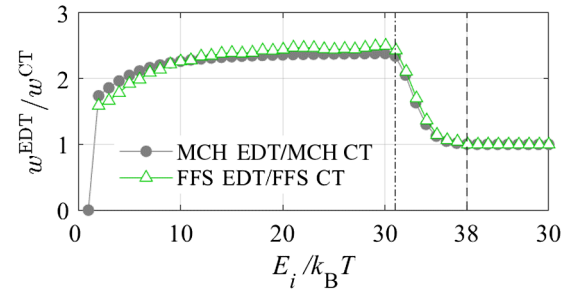

FIG. 4. Ratio of probabilities $w_{i \to i+1}^{\mathrm{EDT}}/w_{i \to i+1}^{\mathrm{CT}}$ for FFS (open triangles) and MCH (full circles) methods as function of the interface energy.

be evaluated for any system with the given barrier ΔE once and for all.

Hence, for evaluating τ_{sw} we have only to collect an accurate statistics of transitions over the effective barrier with the height $\Delta E_{\mathrm{eff}} = b_{\mathrm{room}} k_B T$ using LD with EDT. Corresponding simulation time t_{sim} is not only accessible for the direct LD modeling, but should not grow with the actual barrier ΔE—in strong contrast both to standard LD [where $t_{\mathrm{sim}} \sim \exp(\Delta E/k_B T)$] and to FFS methods ($t_{\mathrm{sim}} \sim \Delta E$). Moreover, our method does not suffer from the instability of multistage methods (see Ref. [28]), because our computation of the product ratio r (4) is error-free.

Physical results and comparison of EDT LD to FFS.— We have simulated with both methods the same series of macrospins with the biaxial anisotropy as in Ref. [27], i.e., having Permalloy magnetic parameters (magnetization $M = 800$ G, damping $\lambda = 0.01$) and demagnetizing factors of flat nanoellipses with the thickness $h = 3$ nm, short axis
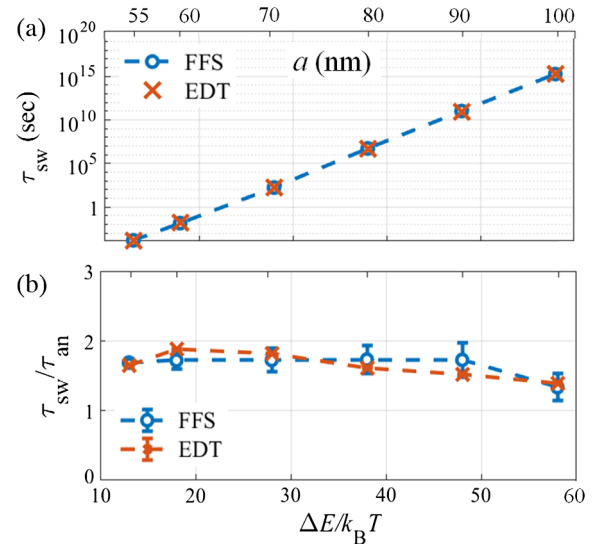

FIG. 5. Switching times computed by FFS (blue circles) and EDT (red crosses) (a) and the same times divided by the analytical result from [27] (b); excellent agreement between FFS and EDT is clearly demonstrated.
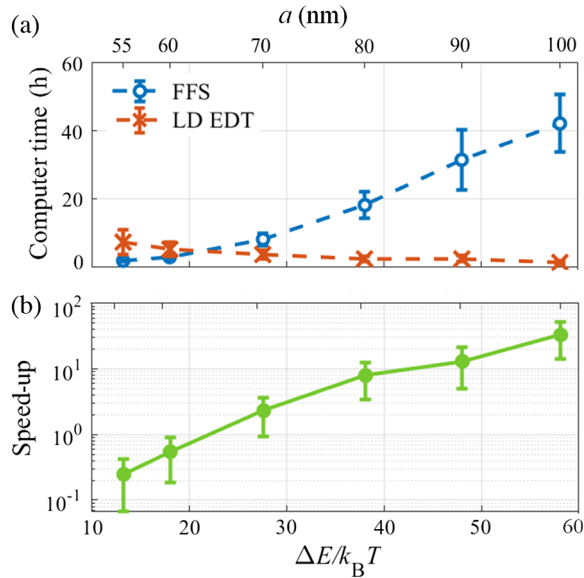
FIG. 6. Computer times (a) and speed-up of the EDT method versus FFS. In both methods, LD with the constant time step $\Delta t = 0.001$ was used to achieve the accuracy of 5% for τ_{sw}.

$b = 40$ nm, and long axes $a = 50 - 100$ nm; corresponding barriers lie in the range $9 \leq \Delta E/k_B T \leq 60$.

Our method shows an excellent agreement with FFS in the whole range of switching times (≈ 20 orders of magnitude; see Fig. 5); it can be seen especially well in Fig. 5(b), where the ratios of FFS and EDT switching times to our analytical result for the same macrospins [27] are plotted.

Finally, to compare the performances of our algorithm and FFS, we have measured simulation times required to compute τ_{sw} with the relative accuracy $\epsilon = 5\%$ by FFS and EDT (Fig. 6). For FFS $t_{\mathrm{sim}} \sim \Delta E$, because the number of interfaces $N \sim \Delta E$. For our EDT method, t_{sim} even decreases with ΔE, because for larger barriers T_{lrg} is higher, facilitating transitions over the barrier [28].

Speed-up of the EDT versus FFS is shown in Fig. 6(b): the break point is achieved already for a very moderate barrier $\Delta E/k_B T \approx 20$, and for the highest studied value $\Delta E/k_B T \approx 60$ EDT is more than 40× faster.

Conclusion.—Introducing the concept of the energy-dependent temperature, we propose a method to compute transition rate over arbitrary high energy barriers by single-stage Langevin dynamics simulations (EDT LD). Verification on biaxial macrospins has shown that EDT LD results agree very well with the forward flux sampling. EDT computation time does not increase with ΔE, in contrast to FFS and analogous algorithms, providing a unique possibility to simulate transitions over any barrier with a very moderate numerical effort. Speed-up of the EDT LD compared to the (strongly optimized) FFS achieves 40× already for $\Delta E \approx 60 k_B T$. Further, EDT does not require the evaluation of the product of a large number of conditional probabilities as in FFS and thus does not suffer from the corresponding instability.

[1] P. Haenggi, P. Talkner, and M. Borkovec, Rev. Mod. Phys. **62**, 251 (1990).
[2] N. van Kampen, *Stochastic Processes in Physics and Chemistry* (Elsevier Science, New York, 1992).
[3] H. Jonsson, G. Mills, and K. Jacobsen, Nudged elastic band method for finding minimum energy paths of transitions, in *Classical and Quantum Dynamics in Condensed Phase Simulations* (World Scientific, Singapore, 1998), Chap. 16, pp. 385–404.
[4] B. Peters, *Reaction Rate Theory and Rare Events* (Elsevier B.V., Amsterdam, 2017).
[5] R. Cabriolu, K. Refsnes, P. Bolhuis, and T. van Erp, J. Chem. Phys. **147**, 152722 (2017).
[6] J. Wales, Annu. Rev. Phys. Chem. **69**, 401 (2018).
[7] S. Hussain and A. Haji-Akbari, J. Chem. Phys. **152**, 060901 (2020).
[8] G. Bussi, A. Laio, and P. Tiwary, Metadynamics: A unified framework for accelerating rare events and sampling thermodynamics and kinetics, in *Handbook of Materials Modeling*, edited by W. Andreoni and S. Yip (Springer Nature, Cham, 2020), Chap. 27, p. 565.
[9] D. Berkov, J. Magn. Magn. Mater. **186**, 199 (1998).
[10] L. Onsager and S. Machlup, Phys. Rev. **91**, 1505 (1953).
[11] W. E, W. Ren, and E. Vanden-Eijnden, Phys. Rev. B **66**, 052301 (2002).
[12] D. Berkov, Magnetization dynamics including thermal fluctuations, in *Handbook of Magnetism and Advanced Magnetic Materials*, edited by H. Kronmüllerand S. Parkin (John Wiley & Sons Ltd, New York, 2007), Vol. 2, Chap. 4, pp. 795–823.
[13] H. Kramers, Physica **7**, 284 (1940).
[14] W. Coffey and Y. Kalmykov, J. Appl. Phys. **112**, 121301 (2012).
[15] V. Mel'nikov and S. Meshkov, J. Chem. Phys. **85**, 1018 (1986).
[16] W. T. Coffey, D. A. Garanin, and D. J. McCarthy, Adv. Chem. Phys. **117**, 483 (2001).
[17] P. M. Déjardin, D. S. F. Crothers, W. T. Coffey, and D. J. McCarthy, Phys. Rev. E **63**, 021102 (2001).
[18] A. Hubert, *Magnetic Domains: The Analysis of Magnetic Microstructures* (Springer-Verlag, Berlin, 1998).
[19] R. J. Allen, P. B. Warren, and P. R. ten Wolde, Phys. Rev. Lett. **94**, 018104 (2005).
[20] R. J. Allen, D. Frenkel, and P. R. ten Wolde, J. Chem. Phys. **124**, 194111 (2006).
[21] E. E. Borrero and F. A. Escobedo, J. Chem. Phys. **129**, 024115 (2008).
[22] R. Allen, C. Valeriani, and P. R. ten Wolde, J. Phys. Condens. Matter **21**, 463102 (2009).
[23] C. Vogler, F. Bruckner, B. Bergmair, T. Huber, D. Suess, and C. Dellago, Phys. Rev. B **88**, 134409 (2013).

[24] C. Vogler, F. Bruckner, D. Suess, and C. Dellago, J. Appl. Phys. **117**, 163907 (2015).

[25] L. Desplat and J.-V. Kim, Phys. Rev. Applied **14**, 064064 (2020).

[26] L. Desplat, C. Vogler, J.-V. Kim, R. L. Stamps, and D. Suess, Phys. Rev. B **101**, 060403(R) (2020).

[27] E. K. Semenova, D. V. Berkov, and N. L. Gorn, Phys. Rev. B **102**, 144419 (2020).

[28] D. Berkov, E. Semenova, and N. Gorn, companion paper, Phys. Rev. B **104**, 224408 (2021).

[29] R. Howard, *Dynamic Probabilistic Systems: Markov Models* (J. Wiley & Sons, New York, 2012).